Synthesis and Characterization of Blue Faceted Anatase Nanoparticles through Extensive Fluorine Lattice Doping

(Article begins on next page)

21 July 2024

iris - AperTO

Synthesis and characterization of faceted anatase nanoparticles through extensive fluorine lattice doping

David G. Calatayud,[†§] Teresa Jardiel,[†] Marco Peiteado,[‡] Francesc Illas[θ], Elio Giamello[φ], Francisco J. Palomares[ᶜ], Daniel Fernández-Hevia[#ᶾ], Amador C. Caballero[†]

[†] Department of Electroceramics, Instituto de Cerámica y Vidrio (CSIC), Kelsen 5, 28049, Madrid, Spain

[‡] POEMMA-CEMDATIC, ETSI Telecomunicación (UPM), Av. Complutense 30, 28040 Madrid, Spain

[θ] Departament de Química Física & IQTCUB, Universitat de Barcelona, C/Martí i Franquès 1, 08028, Barcelona, Spain

[φ] Dipartimento di Chimica and NIS, Università di Torino, Via P. Giuria 7, 10125 Torino, Italy

[ᶜ] Department of Nanostructures and Surfaces, Instituto de Ciencia de Materiales de Madrid, CSIC, c/Sor Juana Inés de la Cruz 3, Campus de Cantoblanco, 28049 Madrid, Spain

[#] Department of Chemistry, Group of Photocatalysis and Spectroscopy Applied to the Environment (FEAM), Universidad de Las Palmas de Gran Canaria, Campus de Tafira, Gran Canaria 35017, Spain

[ᶾ] INAEL Electrical Systems, S.A. c/Jarama 5, Toledo 45007, Spain

ABSTRACT: (Word Style "BD_Abstract"). All manuscripts must be accompanied by an abstract. The abstract should briefly state the problem or purpose of the research, indicate the theoretical or experimental plan used, summarize the principal findings, and point out the major conclusions. Abstract length is one paragraph.

1. INTRODUCTION

Current research endeavors in the field of semiconductor photocatalysts are widely focused on the sustainable production of TiO_2 anatase nanomaterials for environmental purification, hydrogen generation and/or solar energy conversion.[1-5] Among the key parameters boosting the photocatalytic efficiency of anatase nanoparticles, an increased light absorption to extend the optical response to the visible or even the near-infrared region, together with an improved charge separation of the electrons and holes generated upon photoexcitation, shall be enumerated.[6-8] Additionally, given that a variety of physical and chemical processes take place on the surface (viz. adsorption of reactant molecules, surface transfer of photo-excited electrons to reactant molecules, and desorption of product molecules), an enhanced surface reactivity of the TiO_2 particles will be paramount too for the photocatalytic performance of these materials.[9-10] A careful look to the specialized literature reveals that the problems with the surface reactivity are in the process of being solved. Working on the processing strategy, a collective exposition of the three fundamental low-index facets of TiO_2 anatase crystals can be more or less ensured to yield a more efficient photocatalytic response.[11-15] So far, the best scenario has been found when employing fluorine-based compounds as dopants, since fluorine atoms can act as both morphology directors and electron scavengers to reduce the recombination rate of electrons and holes.[16-21] However the produced F-doped anatase materials still fail to meet some crucial engineering requirements, exhibiting a too poor behavior in the visible region. Several factors may account for this inconvenience, but undoubtedly the band structure of TiO_2 anatase is decisive. TiO_2 anatase has a bandgap of 3.2 eV which only allows the excitation of carriers by light with wavelengths smaller than 387 nm; if visible light harvesting is to be enabled, this gap should be narrowed. Chemical doping is known as an effective method to narrow the bandgap, and fluorine, in particular, should be a good candidate cause it can modulate the valence band of TiO_2.[22,23] Up to date, however, most attempts to reduce the band gap of anatase through fluorine doping has resulted little operative. Now there is evidence that this debacle could be attributed to the doping process itself, or to be more precise, to the magnitude of the doping process: the synthetic processes employed to prepare F-doped anatase more or less succeed in attaining a functional surface doping of the TiO_2 nanoparticles, but an effective F-doping of the TiO_2 lattice is more difficult to guarantee. For example, in a previous work we developed a one-step semi solvothermal methodology in which by using trifluoroacetic acid (TFAA) as both capping agent and electron scavenger, highly crystalline anatase nanoparticles with an upgraded photocatalytic response were successfully prepared.[24] As we attested, fluorine primarily adsorbs on the surface of the TiO_2 nanoparticles either through the oxygen atoms of the TFAA molecule itself or as fluorine ions released from the partial decomposition of TFAA. That is to say, the incorporated fluorine species firmly modify the surface of the anatase nanoparticles and

improve their photoreactivity, but actually a bulk homogeneous doping of the crystal lattice is not really accomplished. As a straight consequence the band gap of the produced nanoparticles barely changes from that of pure TiO₂. Feasibly, an effective F-doping of the TiO₂ lattice will produce a different score, but then the following question must be responded: is it really possible to achieve such uniform lattice doping?

Theoretical premise

To answer this question we have executed some periodic density functional calculations, mostly aimed to figure out if fluorine atoms can indeed enter the anatase structure and how they do it. In a first series of calculations,[25] the thermodynamic stability of F-doped anatase was investigated using large enough supercells; these are needed to guarantee that the dopant concentration in the computational models (~1%) is close (or not too far) from the values in the experimental samples. The results revealed that substitutional (O by F) F doping of bulk anatase, but also of rutile and brookite, is always thermodynamically favored. In order to investigate how F can reach appropriate sites of bulk TiO₂ anatase, F diffusion through the material was also considered using a similar approach.[26] Results consistently showed that, in the case of anatase, the strong relaxation of the substrate in response to the presence of the dopant leads to relatively small energy barriers for diffusion which, in the case of the [100] direction appears to almost vanish. Consequently, F-doping is thermodynamically favored and the presence of F in the vicinity of O sites in the bulk of anatase becomes possible thanks to the low energy barriers for diffusion. Obviously, diffusion can only start once the corresponding surfaces are fully covered with F. Again, the density functional calculations show that F adsorption is exothermic and that the presence of F has a differential effect on the different surfaces, stabilizing the more reactive (001) surface and destabilizing the more stable (in absence of F) (101) surface.[27] To summarize, the periodic density functional calculations strongly suggest that F doping is possible and the mechanism involves surface covering and diffusion through the bulk. In this way, F at the surface and at interstitial sites during diffusion provides a reservoir for O substitution by F which can be used in other processes.

Now looking back to our synthesis methodology, we have identified one key feature which may explain the difficulties to effectively dope the anatase lattice: as witnessed by XPS and FTIR measurements[24] a considerable number of TFFA molecules remains unabridged after the solvothermal process and, consequently, the amount of free fluorine ions to enter the TiO₂ lattice is eventually too low. Our previous experience with this system suggests that increasing the amount of TFFA added to the starting pot essentially leads to unwelcome morphologies, poorly faceted anatase nanoparticles and/or broadened size distributions. Conversely, when introducing subtle changes in the experimental conditions, the degradation of the TFAA molecule can be encouraged without altering the targeted crystal growth habit. In particular the greatest scores have come when shifting the temperature of the solvothermal process.

As indicated, the introduced change had to be fairly smooth: the maximum temperature was slightly increased from 200 to 235 °C, but as results will here demonstrate this is fairly enough to largely degrade the TFFA, to increase the amount of released fluorine ions that could enter the TiO₂ lattice and, eventually, to successfully reduce the bandgap of TiO₂.

2. EXPERIMENTAL

Synthesis of TFAA-modified anatase TiO₂ nanoparticles (Ti-TFAA). Well-faceted nanoparticles of TiO₂ have been synthesized through a one-step semi-solvothermal route using as received titanium(IV) tetrabutoxide (Ti(OBut)₄, Fluka, 98%) and trifluoroacetic acid (CF₃COOH, Aldrich, 70%, TFAA). Compared with other alkyl precursors, the butoxide group of Ti(OBut)₄ exhibits a slower rate of hydrolysis, thereby allowing an enhanced control of the diffusion and polymerization processes.[24] In a typical procedure 5 ml of Ti(OBut)₄ are introduced in a 50 ml Teflon-lined stainless steel autoclave, together with 1.9 g of TFAA. A small amount of deionized water (0.4 ml) is added to accelerate the hydrolysis reaction. The system is then heated at 235 °C for 24 h. The obtained blue precipitate (Figure 1 a) is washed several times with water and ethanol (96%) and then dried at 105 °C.

Processing and characterization methods. A comprehensive examination of the obtained Ti-TFAA powders was conducted using a broad set of characterization techniques. The analyses of the crystalline structure and the phase identification were performed by X-ray diffraction (XRD Bruker D8 ADVANCE, Madison, WI, USA) with a monochromatized source of Cu-Kα1 radiation (λ = 1.5406 nm) at 1.6 kW (40 KV, 40 mA); samples were prepared by placing a drop of a concentrated ethanol dispersion of particles onto a single crystal silicon plate. Transmission electron microscopy (TEM) images were obtained on a JEOL 2100 F TEM/STEM (Tokyo, Japan) operating at 200 kV and equipped with a field emission electron gun providing a point resolution of 0.19 nm; samples were prepared by placing a drop of a dilute ethanol dispersion of nanoparticles onto a 300-mesh carbon-coated copper grid and evaporated immediately at 60 °C.

X-ray photoelectron spectroscopy (XPS) was used to characterize the chemical composition of the samples. XPS spectra were acquired in an ultrahigh vacuum (UHV) chamber with a base pressure of 1 × 10−9 mbar using a hemispherical electron energy analyzer (SPECS Phoibos 150 spectrometer) and a monochromatic AlKα X-ray source (1486.74 eV). XPS spectra were recorded at the normal emission take-off angle, using an energy step of 0.05 eV and a pass-energy of 10 eV for high resolution data, which provides an overall instrumental peak broadening of 0.4 eV.[xx] Carbon and hydroxyl (OH) species were also detected as surface contaminants and the signal from adventitious carbon at 284.6 eV was used for energy calibration. Data processing was performed using CasaXPS software.

The infrared spectra of the samples were obtained on Fourier transform infrared spectrometer Thermo Nicolet

6700 FTIR equipment by using the Attenuated Total Reflectance (ATR) method (polyethylene detector). The obtained spectra were averaged from a minimum of 512 scans.

Electron Paramagnetic Resonance (EPR) spectra, recorded either at room temperature or at liquid nitrogen temperature (77K), were run on a X-band CW-EPR Bruker EMX spectrometer equipped with a cylindrical cavity operating at 100 kHz field modulation.

3. RESULTS

The first evidence of a different scenario after modifying the synthesis conditions was found in the color of the obtained powder. In the preceding experiment conducted at 200 °C, the dried precipitate was initially brown colored and it had to be cleaned under UV-vis irradiation to remove the unreacted organic matter; a white powder was then obtained.[24] Now, the increase in the reaction temperature produces a blue powder after drying the precipitate, with no need for further cleaning (Figure 1 a). This bluish tone has been already related to the occurrence of Ti^{3+} centers in reduced TiO_2;[28-31] in some of these previous experiments, however, the blue color irrevocably disappears after further annealing or after a long air exposure, indicating a reversible $Ti^{4+} \leftrightarrow Ti^{3+}$ redox process.[31] In the present sample no such loss of the blue color is observed; moreover, although an aggressive treatment with H_2O_2 to oxidize the surface initially turns the precipitate to yellow shade (Figures 1 b and c), several days after removing the peroxide the blue color is completely spontaneously recovered (Figure 1 d).
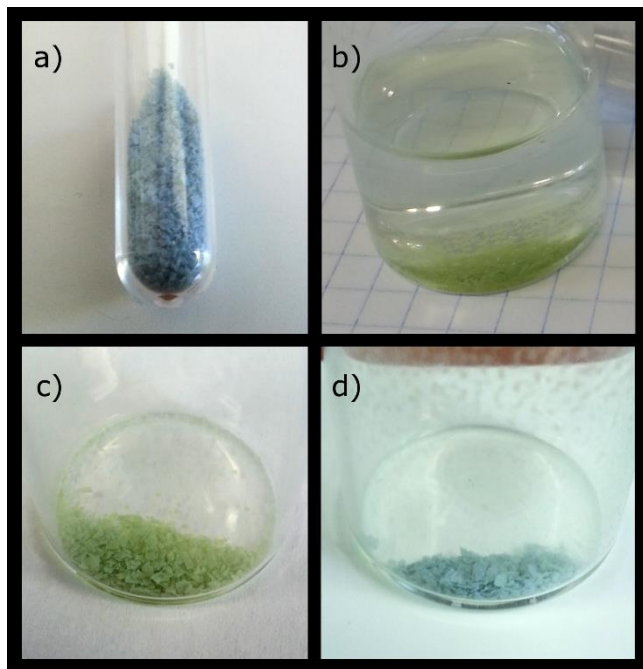

Figure 1. Image of: a) the TiO_2 blue synthesized powder, b) TiO_2 Blue with H_2O_2, c) TiO_2 Blue after the treatment with H_2O_2 and d) TiO_2 Blue treated with H_2O_2 after several days.

The crystal structure of the blue powder was investigated by X-ray diffraction (Figure 2). As happened with the sample synthesized at 200 °C, a crystalline single-phase pattern corresponding to TiO_2 anatase was obtained (ICDD file no. 21-1272) with no perceivable traces of the rutile polymorph. Actually, to the eye of XRD the increase in temperature merely returns a slim narrowing of the anatase peaks, indicating a slightly enhanced crystallinity in the particles of the new experiment (consistent with the higher temperature).
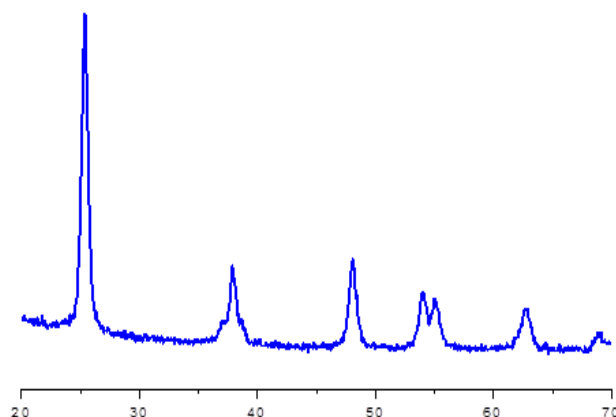
Figure 2. X-ray diffraction pattern for the synthesized Ti-Blue powder. All peaks corresponding to the anatase TiO_2 phase.

Further structural characterization was conducted by High Resolution TEM. Images in Figure 3 reveal the presence of well-faceted nanocrystals (15-20 nm) with broadly truncated rhombic shapes, again showing no big difference with the particles obtained at 200 °C. Interestingly, the rhombic shapes are consistent with Wulf type anatase nanoparticles exhibiting {101} and {001} facets.
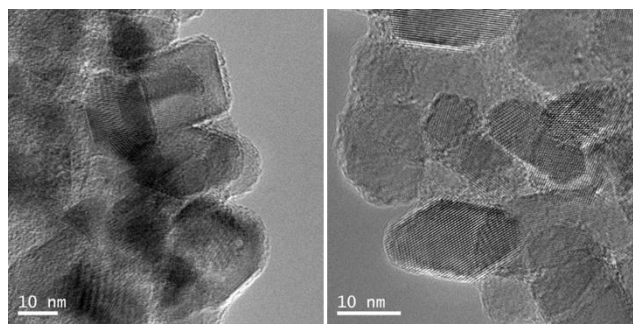

Figure 3. TEM micrographs of the anatase nanoparticles Ti-Blue with different orientations.

Figure 4 depicts the results of the FTIR analyses performed on both, previous and present, experiments. At first glance the two spectra show the same shape of the base-line and the same characteristic bands, so in general terms we may presume a similar picture to that already discerned for the sample treated at 200 °C: bonded through the oxygen atoms of the carboxylic group, the TFAA molecules reside chemisorbed on the surface of the TiO_2 crystals mainly in a bidentate mode.[24] But looking thoroughly to the intensity of the recorded IR bands, there is now one

sizeable difference between both samples, which is particularly significant for those bands assigned to TFFA: the C=O stretching vibrations at 1634 and 1442 cm^{-1} and the C-F stretching vibrations at 1204 and 1158 cm^{-1} exhibit a lower intensity when the sample is treated at 235 °C. Such diminution basically indicates a lower amount of TFAA adsorbed at the surface of the TiO$_2$ particles which, in turn, could obey to a larger decomposition of the TFFA molecule with the higher temperature.
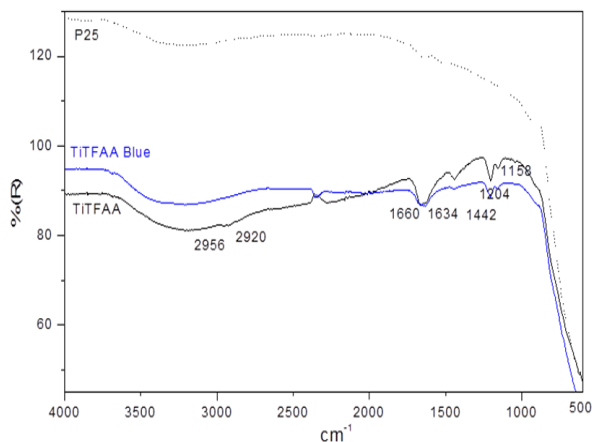
**Figure 4.** FTIR spectra of the TiO$_2$ blue powder, TiTFAA and P25.

High resolution XPS analyses in Figure 5 correspond to the F$_1$s core level photoemission of both samples and as depicted two main components are easily discriminated: the C-F component, which can be mostly related to –CF$_3$ groups of the TFAA molecule adsorbed on the surface of the TiO$_2$ particles, and the Ti-F component ascribed to the adsorption of free fluorine atoms.[19,32-34] Visibly the proportion between these two components has decreased for the blue precipitate obtained at 235 °C, indicating either a lower amount of -CF$_3$ groups or a higher quantity of free fluorine atoms; whatever predominates, both cases again point towards a larger degradation of TFAA with the intended increment in the reaction temperature.
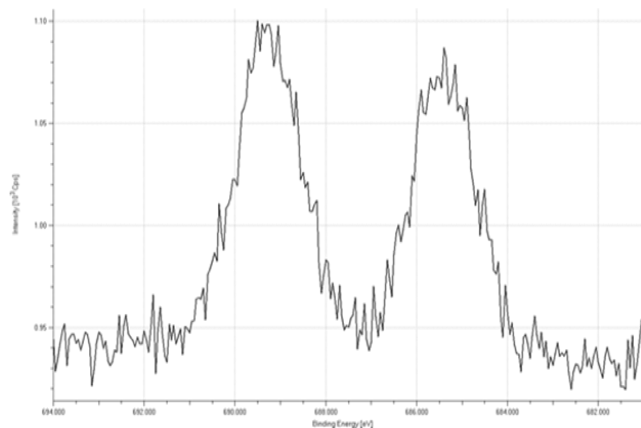
Figure 5. High resolution XPS spectrum corresponding to F$_1$s region for the Ti-Blue sample.

Electron magnetic resonance and optical characterization

As indicated above the occurrence of the blue colour in the powder obtained at 235 °C may be ascribed to the presence of Ti^{3+} centres in the anatase lattice. To verify this point we have conducted EPR measurements. X-band CW-EPR spectra of the sample were recorded at room temperature and at 77 K in air and under vacuum. The spectra are reported in Figure 6 (a-c).
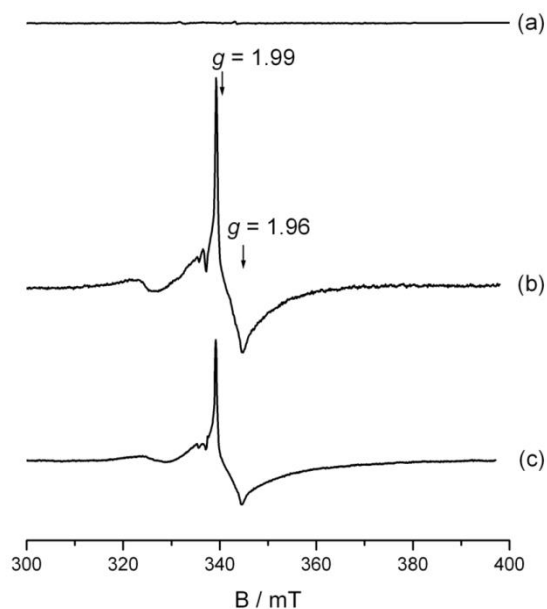
Figure 6. X band CW-EPR spectra of the as prepared Ti-TFAA sample recorded in air at room temperature (a) and at 77 K (b). Line (c) reports the spectrum of the same material recorded at 77 K under vacuum.

At room temperature the base line of the EPR spectrum is flat (Figure 6a) and no trace of paramagnetic species is observed in such conditions. Lowering the temperature to 77 K an intense EPR signal shows up at g values lower than the free electron value (Figure 6b). The structure of the spectrum (which is clearly appreciable in spite of the wide linewidth) is axial with g$_\perp$=1.992, g$_{//}$=1.962. These features of the g tensor are typical of Ti^{3+} ions in octahedral-type symmetry. The spectrum does not change significantly upon outgassing the sample (Figure 6c). The observed g tensor values are the same found in other cases of modified anatase powders. In particular, in the case of previously reported EPR studies of fluorine doped TiO$_2$ samples the same axial spectrum was observed though with narrower linewidth due to the low concentration of Ti^{3+} centers.[35] The spectra reported in Figure 6 are thus amenable to the presence of Ti^{3+} centers in the solid. The absence of a spectral trace at room temperature could be due to charge detrapping at elevated temperature. However this interpretation remains an hypothesis since most Ti^{3+} signal vanish at temperatures near RT because of their intrinsic relaxation time. The large linewidth observed for the spectra in Figure 6 is due to the relatively high concentration of such

centers which causes dipolar broadening of the spectral line. This is confirmed comparing the spectra with those reported in the literature36 and generated by annealing under vacuum at increasing temperature an F-doped TiO_2 sample. The starting spectrum observed for the as pre-pared material is, as mentioned before, the same spectrum here reported with $g_\perp=1.992$ and $g_{//}=1.962$ but with narrow linewidth. Annealing under vacuum causes a progressive loss of oxygen, with the consequent formation of excess electrons in the solid which are stabilized as Ti^{3+} centres. The effect observed upon annealing36 is therefore a pro-gressive growth of the spectral intensity (the concentration of Ti^{3+} increases) paralleled by broadening of the signal (onset of dipolar interactions) which eventually assumes a shape strictly similar to that of the spectra in Figure 6. There is therefore no doubt that the EPR spectra here re-ported are due to Ti^{3+} centers typical of the bulk anatase lattice (see the Discussion Section). At variance with pre-viously reported cases of F-doped TiO_2, here the ~~starting~~ material already contains a relevant concentration of re-duced Ti centers as stated also by its optical absorption in the visible region which is absent in the materials with low F concentration.

Finally Figure 7 depicts the UV-vis diffuse reflectance spectra for both, white and blue, powders. As a tangible difference an onset of visible and NIR absorption occurs in the blue sample which is, however, not observed for the white sample. The band gap value was estimated from the corresponding Tauc plot (($\alpha h v)^{1/2}$ vs hv). As illustrated while the absorption edge of the white powder yields a band gap of 3.20 eV, the accepted value for TiO_2 anatase, the blue precipitate displays an exceptional lower bandgap of 3.01 eV.

4. DISCUSSION

FTIR and XPS analyses both suggest that the increase in the synthesis temperature of the solvothermal reaction neatly provokes an increased degradation of the starting TFAA. Eventually this leads to a fine-tuning of the anatase electronic structure which is evidenced by the stable blue colour of the as-obtained powders and, behind this, by the formation of a large number of EPR-visible Ti^{3+} centres. In-deed, the following two major mechanisms can account for the formation of the bulk Ti^{3+} ions in these samples: On one hand the higher degradation of TFAA first produces a higher release of free fluorine ions to the medium, which substantially increases the doping capacity of the reacting system. Fluorine substitutes oxygen in the lattice and Ti^{3+} centres are then formed via a mechanism of valence induc-tion whereby a fraction of the extra-electrons borne by flu-orine is stabilized by Ti cations. The resulting composition of the solid can be written as $Ti^{4+}_{(1-x)}Ti^{3+}_xO^{2-}_{(2-x)}F^-_x$. Moreo-ver, EPR measurements unambiguously indicate that those excess electrons are specifically localized (stabilized) by regular lattice Ti^{4+} cations of the oxide bulk: the axial signal with components at $g_\perp=1.992$ and $g_{//}=1.962$ appears when titania is doped with elements bearing an extra-electron with respect to Titanium and Oxygen (this is the case also

of pentavalent metallic elements such as niobium or anti-mony)[36] or when electrons are injected in mild conditions by contact with reactive elements such as atomic hydrogen or alkaline metals.[38] Since the signal here reported is typi-cal of the unperturbed solid (signals obtained with bare an-atase by other reduction methods have different features) it must be associated to the regular crystallographic site typical of the anatase bulk;[38,39] this assignment is also cor-roborated by theoretical investigations.[40]

Additionally, the higher degradation of the TFAA or-ganic molecules also produces a highly reducing atmos-phere within the material during the solvothermal process. Titanium dioxide is a reducible compound whose compo-sition greatly depends on the oxygen pressure. Therefore a reducing atmosphere will tangibly encourage the for-mation of Ti^{3+} reduced species and the fact is that when HF is used as the fluorine source no such atmosphere is cre-ated (no organic matter being degraded) and, conse-quently, the number of Ti^{3+} centers is clearly lower as evi-denced by EPR analyses.[36]

In other words, all EPR results previously reported con-cerning F-doped titania show the same signals here re-ported but with much narrower linewidth.[35,36] Since the line intensity and the large linewidth observed in the pre-sent case correspond to a higher number of reduced Ti^{3+} centers exhibiting mutual dipolar interaction, it can easily be concluded that the synthetic method here illustrated is much more efficient than those reported before in intro-ducing fluorine ions into the lattice of anatase.
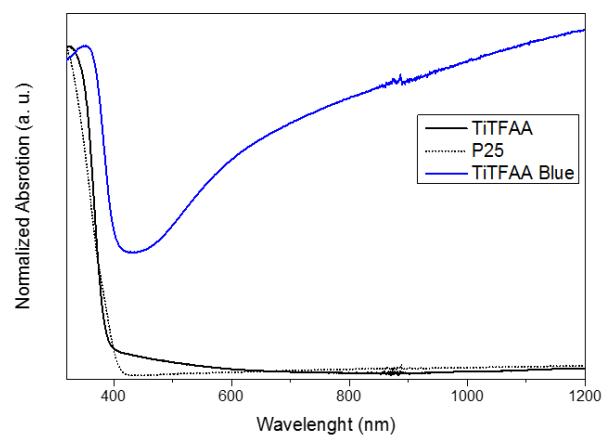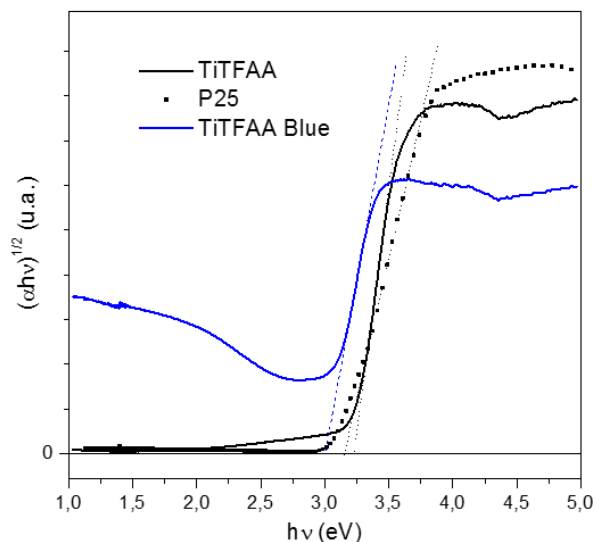
Figure 7. a) DR UV–vis–NIR spectra and b) Tauc plot from the UV-vis absorption spectra corresponding to the Ti-Blue, TiTFAA and P25.

Obviously this extensive fluorine doping of the anatase lattice and the subsequent formation of a large number of Ti^{3+} centers will depict the optoelectronic behavior of the doped material: As it has been demonstrated the energy levels corresponding to the Ti^{3+} reduced states are extremely shallow;[36] the excess electrons tend to be delocalized over several of these Ti centers and consequently the Fermi level lies at the boundary or even in the lower region of the conduction band. When the concentration of Ti^{3+} states is greatly increased, as in our case, a sort of sub-band is formed close to the bottom of the conduction band, eventually resulting in a small but clear red shift of the optical band gap transition, i.e., in a decrease of the band gap (almost 0.2 eV from that of pristine anatase). The broad absorption peak (Fig. 7), having a maximum in the IR region and tailing into the visibile one (which is the reason of the blue color assumed by the F doped samples) indeed indicates the presence of free carriers inside the solid [L. De Trizio, R Buonsanti, A. M. Schimpf, A. Llordes, D. R. Gamelin, R. Simonutti, D. J. Milliron, Nb-Doped Colloidal TiO_2 Nanocrystals with Tunable Infrared Absorption, Chem. Mater. 2013, 25, 3383−3390,

Xxx Komenko et al see references]

.,
Photocatalytic performance

The highly faceted morphology of the synthesized F-doped anatase nanoparticles together with the improved doping capability of the system eventually allows and enhanced UV photocatalytic performance. Figure 8 shows such photoactivity upon the degradation of methyl orange, evidencing how the change from a surface doped material (TiTFAA) to a lattice doped one (Ti-Blue) undeniably provokes a faster response; moreover, it is clearly faster than that of Degussa P25 TiO_2 commercial catalyst, and gets closer to that of Kronos, another commercial catalyst based on TiO_2 but doped with Carbon instead of Fluorine.
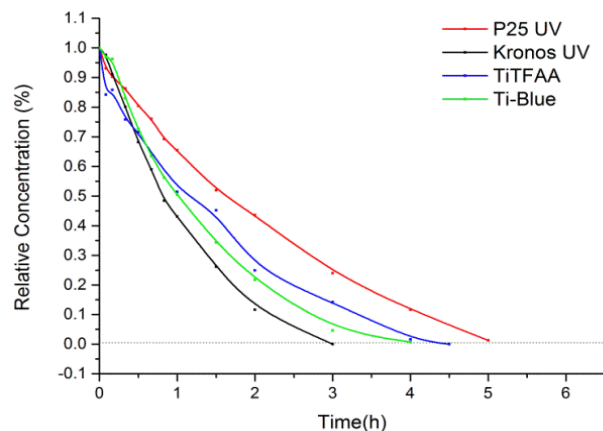
Figure 8. Evolution with the reaction time of methyl orange for the Ti-Blue, Ti-TFAA, P25 and Kronos photocatalysts under UV light.

But as described, the higher incorporation of Fluorine ions into the anatase lattice also provokes the observed reduction in the bandgap of TiO_2, which now falls in the vicinity of the visible region: 3.01 eV. According to this value, an improved visible-light response of the produced nanoparticles would be expected. However we have carried out some additional photocatalytic experiments which, unfortunately, indicated that a substantial improvement in the solar energy conversion is still hindered.
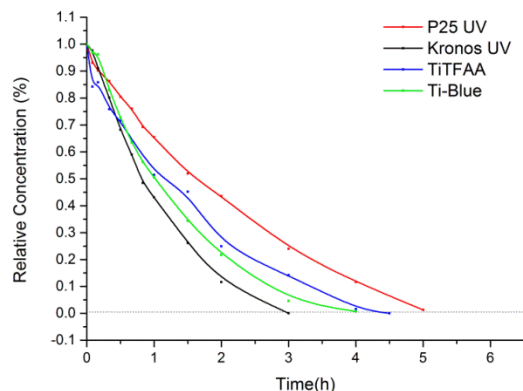
Figure 9. Evolution with the reaction time of methyl orange for the Ti-Blue, Ti-TFAA, P25 and Kronos photocatalysts under visible light.

More specifically Figure 9 compares the activity of our blue powder with the other three photocatalysts on the degradation of methyl orange under visible light. The fact is that these three other powders, P25, Kronos and our previous TiTFAA they all have a bandgap around 3.2 eV but as observed, the narrower bandgap of the blue titania is not clearly leading to a better visible light harvesting. Actually this unfavourable behaviour has been already observed and attributed to an undesirably fast charge recombination occurring at the dopant centers, impeding the charge transfer from bulk to the surface and hence restraining the photocatalytic performance.[41] A clear conclusion from the present findings is that the existence of a narrower band

gap does not necessarily lead to a better photocatalytic performance under visible light, a fact which has also been highlighted in the literature.

5. CONCLUSIONS

Highly crystalline fluorine-doped anatase nanoparticles have been prepared applying a modified one-step semi solvothermal methodology which also allows a more effective doping process, changing from a surface doped material to a lattice doping scenario. This is evidenced by the great number of Ti^{3+} centers occurring in the material, which mainly form to stabilize the extra electrons produced when fluorine substitutes oxygen in the TiO_2 lattice. As a first consequence the obtained blue powders exhibit an improved UV photocatalytic response. But more interestingly, upon lattice doping, the electronic structure of anatase TiO_2 is also fine-tuned and eventually its bandgap is narrowed making it closer to the visible region. Initially this remarkable result would open the doors for an increased solar energy conversion; unfortunately a fast charge recombination is likely to happen at these dopant centers which still hinders the visible light harvesting, so new experiments must be envisaged to prevent or at least reduce that charge recombination process while preserving the reduced bandgap.

ASSOCIATED CONTENT

Supporting Information. A brief statement in nonsentence format listing the contents of material supplied as Supporting Information should be included, ending with "This material is available free of charge via the Internet at http://pubs.acs.org." For instructions on what should be included in the Supporting Information as well as how to prepare this material for publication, refer to the journal's Instructions for Authors.

AUTHOR INFORMATION

Corresponding Author

* (Word Style "FA_Corresponding_Author_Footnote"). Give contact information for the author(s) to whom correspondence should be addressed.

Present Addresses

§ Present address: Department of Chemistry, University of Bath, Claverton Road, BA2 7AY, Bath, UK.

Author Contributions

The manuscript was written through contributions of all authors. / All authors have given approval to the final version of the manuscript. / ‡These authors contributed equally. (match statement to author names with a symbol)

Funding Sources

Any funds used to support the research of the manuscript should be placed here (per journal style).

Notes

Any additional relevant notes should be placed here.

ACKNOWLEDGMENT

ABBREVIATIONS

CCR2, CC chemokine receptor 2; CCL2, CC chemokine ligand 2; CCR5, CC chemokine receptor 5; TLC, thin layer chromatography.

REFERENCES

(Word Style "TF_References_Section"). References are placed at the end of the manuscript. Authors are responsible for the accuracy and completeness of all references. Examples of the recommended formats for the various reference types can be found at http://pubs.acs.org/page/4authors/index.html. Detailed information on reference style can be found in The ACS Style Guide, available from Oxford Press.

(1) Xu, H.; Ouyang, S.; Liu, L.; Reunchan, P.; Umezawa, N.; Ye, J. Recent Advances in TiO2-based photocatalysis. *J. Mater. Chem. A* **2014**, 2, 12642-falta.

2. R. Asahi, T. Morikawa, T. Ohwaki, K. Aoki, Y. Taga. "Visible-light photocatalysis in nitrogen-doped titanium oxides", Science 293, 269-271 (2001).

3. S.U.M. Khan, M. Al-Shahry, W.B. Ingler. "Efficient photochemical water splitting by a chemically modified n-TiO2", Science 297, 2243-2245 (2002).

4. X. Chen, L. Liu, P.Y. Yu, S.S. Mao. "Increasing solar absorption for photocatalysis with black hydrogenated titanium dioxide nanocrystals", Science 331, 746-750 (2011).

5. M. Setvin, U. Aschauer, P. Scheiber, Y.F. Li, W. Hou, M. Schmid, A. Selloni, U. Diebold. "Reaction of O2 with subsurface oxygen vacancies on TiO2 anatase (101)", Science 341, 988-991 (2013).

6. H. Tong, S. Ouyang, Y. Bi, N. Umezawa, M. Oshikiri, J. Ye. "Nano-photocatalytic materials: Possibilities and challenges" Adv. Mater. 24, 229-251 (2012).

7. X. Pan, M.Q. Yang, X. Fu, N. Zhang, Y.J. Xu. "Defective TiO2 with oxygen vacancies: Synthesis, properties and photocatalytic applications", Nanoscale 5, 3601-3614 (2013).

8. Y. Wang, Q. Wang, X. Zhan, F. Wang, M. Safdar, J. He. "Visible light driven type II heterostructures and their enhanced photocatalysis properties: A review", Nanoscale 5, 8326-8339 (2013).

9. H.G. Yang, C.H. Sun, S.Z. Qiao, J. Zou, G. Liu, S.C. Smith, H.M. Cheng, G.Q. Lu. "Anatase TiO2 single crystals with a large percentage of reactive facets", Nature 453, 638-641 (2008).

10. S. Liu, J. Yu, M. Jaroniec. "Anatase TiO2 with dominant high-energy {001} facets: Synthesis, properties, and applications", Chem. Mater. 23, 4085-4093 (2011).

11. C.Z. Wen, H.B. Jiang, S.Z. Qiao, H.G. Yang, G.Q. Lu. "Synthesis of high-reactive facets dominated anatase TiO2", J. Mater. Chem. 21, 7052-7061 (2011).

12. L. Ye, J. Mao, J. Liu, Z. Jiang, T. Peng, L. Zan. "Synthesis of anatase TiO2 nanocrystals with {101}, {001} or {010} single facets of 90% level exposure and liquid-phase photocatalytic reduction and oxidation activity orders", J. Mater. Chem. A 1, 10532-10537 (2013).

13. J. Pan, G. Liu, G.Q. Lu, H.M. Cheng. "On the true photoreactivity order of {001}, {010}, and {101} facets of anatase TiO2 crystals" Angew. Chem. Int. Ed. 50, 2133-2137 (2011).

14. S. Selçuk, A. Selloni. "Surface structure and reactivity of anatase TiO2 crystals with dominant {001} facets", J. Phys. Chem. C 117, 6358-6362 (2013).

15. G. Liu, J. Yu, G.Q. Lu, H.M. Cheng. "Crystal facet engineering of semiconductor photocatalysts: Motivations, advances and unique properties", Chem. Commun. 47, 6763-6783 (2011).

16. V. Maurino, C. Minero, G. Mariella, E. Pelizzetti. "Sustained production of H2O2 on irradiated TiO2-Fluoride systems", Chem. Commun. 2627-2629 (2005).

17. K. Lv, Y. Xu. "Effects of polyoxometalate and fluoride on adsorption and photocatalytic degradation of organic dye X3B on TiO2: The difference in the production of reactive species", J. Phys. Chem. B 110, 6204-6212 (2006).

18. Y. Xu, K. Lv, Z. Xiong, W. Leng, W. Du, D. Liu, X. Xue. "Rate enhancement and rate inhibition of phenol degradation over irradiated anatase and rutile TiO2 on the addition of NaF: New insight into the mechanism", J. Phys. Chem. C 111, 19024-19032 (2007).

19. X. Meng, L. Qi, Z. Xiao, S. Gong, Q. Wei, Y. Liu, M. Yang, F. Wang. "Facile synthesis of direct sunlight-driven anatase TiO2 nanoparticles by in situ modification with trifluoroacetic acid", J. Nanopart. Res. 14, 1176 (2012).

20. S.C. Padmanabhan, S.C. Pillai, J. Colreavy, S. Balakrishnan, D.E. McCormack, T.S. Perova, Y. Gun'ko, S.J. Hinder, J.M. Kellys. "A simple sol-gel processing for the development of high-temperature stable photoactive anatase titania", Chem. Mater. 19, 4474-4481 (2007).

21. K. Lv, B. Cheng, J. Yu, G. Liu. "Fluorine ions-mediated morphology control of anatase TiO2 with enhanced photocatalytic activity", Phys. Chem. Chem. Phys. 14, 5349-5362 (2012)

22. J. C. Yu, J. G. Yu, W. K. Ho, Z. T. Jiang, L. Z. Zhang. "Effects of F- doping on the photocatalytic activity and microstructures of nanocrystalline TiO2powders", Chem. Mater. 14, 3808-3816 (2002).

23. W. Q. Fang, X. L. Wang, H. M. Zhang, Y. Jia, Z. Y. Huo, Z. Li, H. J. Zhao, H. G. Yang, X. D. Yao. "Manipulating solar absorption and electron transport properties of rutile TiO2 photocatalysts via highly n-type F-doping", J. Mater. Chem. A 2, 3513-3520 (2014).

24. D.G. Calatayud, T. Jardiel, M. Peiteado, C. Fernandez, M. Rocio, J.M. Dona, F.J. Palomares, F. Rubio, D. Fernandez, A.C. Caballero. "Highly photoactive anatase nanoparticles obtained using trifluoroacetic acid as an electron scavenger and morphological control agent", J. Mater. Chem. A 1, 14358-14367 (2013).

25. S. Tosoni, O. Lamiel-Garcia, D. Fernandez-Hevia, J. M. Doña, F. Illas. "Electronic structure of F-doped bulk rutile, anatase and brookite polymorphs of TiO2", J. Phys. Chem. C 116, 12738-12746 (2012).

26. S. Tosoni, O. Lamiel Garcia, D. Fernandez Hevia, F. Illas. "Theoretical Study of Atomic Fluorine Diffusion through Bulk TiO2 Polymorphs", J. Phys. Chem. C 117, 5855-5860 (2013)

27. O Lamiel-Garcia, S. Tosoni, F. Illas. "Relative stability of F covered TiO2 anatase (101) and (001) surfaces from periodic DFT calculations and ab initio atomistic thermodynamics", J. Phys. Chem. C 118, 13667-13673 (2014).

28. U. Diebold, M. Li, O. Dulub, E.L.D. Hebenstreit, W. Hebenstreit. "The relationship between bulk and surface properties of rutile TiO2(110)", Surf. Rev. Lett. 5–6, 613–617 (2000).

29. E. Carter, A.F. Carley, D.M. Murphy. "Evidence for O2– radical stabilization at surface oxygen vacancies on polycrystalline TiO2", J. Phys. Chem. C 111, 10630–10638 (2007).

30. N.A. Deskins, M. Dupuis. "Intrinsic hole migration rates in TiO2 from density functional theory", J. Phys. Chem. C, 113, 346–358 (2009).

31. E.M. Hopper, F. Sauvage, A.K. Chandiran, M. Grätzel, K.R. Poeppelmeier, T.O. Mason. "Electrical properties of Nb-, Ga-, and Y-substituted nanocrystalline anatase TiO2 prepared by hydrothermal synthesis", J. Am. Chem. Soc. 95, 3192–3196 (2012).

32. X.H. Yang, Z. Li, C. Sun, H.G. Yang, C. Li. "Hydrothermal stability of {001} faceted anatase TiO2", Chem. Mater. 23, 3486-3494 (2011).

33. C. Ni, Z. Zhang, M. Wells, T.P. Beebe Jr., L. Pirolli, L.P. Méndez De Leo, A.V. Teplyakov. "Effect of film thickness and the presence of surface fluorine on the structure of a thin barrier film deposited from tetrakis-(dimethylamino)-titanium onto a Si(100)-2×1 substrate", Thin Solid Films 515, 3030-3039 (2007).

34. M. Senna, V. Sepelak, J. Shi, B. Bauer, A. Feldhoff, V. Laporte, K.D. Becker. "Introduction of oxygen vacancies and fluorine into TiO2 nanoparticles by co-milling with PTFE", J. Solid State Chem. 187, 51-57 (2012).

35. A. Czoska, S. Livraghi, M. Chiesa, E. Giamello, S. Agnoli, G. Granozzi, E. Finazzi, C. Di Valentin, G. Pacchioni. "The Nature of Defects in Fluorine-Doped TiO2", J. Phys. Chem. C, 1122, 8951 (2008).

36. J. Biedrzycki, S. Livraghi, E. Giamello, S. Agnoli, G. Granozzi. "Fluorine and Niobium doped TiO2: chemical and spectroscopic properties of polycrystalline n-type doped anatase", J. Phys. Chem. C 118,8462 (2014).

38. S. Livraghi, M. Chiesa, M.C. Paganini and E. Giamello. "On the Nature of Reduced States in Titanium Dioxide As Monitored by Electron Paramagnetic Resonance. I: The Anatase Case", J. Phys. Chem. C 115, 25413 (2011).

39. M. Chiesa, S. Livraghi, M.C. Paganini, E. Giamello. "Charge trapping in TiO2 polymorphs as seen by Electron Paramagnetic Resonance Spectroscopy", Phys.Chem. Chem. Phys. 15, 9435 (2013).

40. C. Di Valentin, G. Pacchioni and A. Selloni. "Reduced and n-Type Doped TiO2: Nature of Ti3+ Species", J. Phys. Chem. C 113, 2053 (2009)

41. C. Zhang, S. Chen, L.E. Mo, Y. Huang, H. Tian, L. Hu, Z. Huo, S. Dai, F. Kong, X. Pan. "Charge recombination and band-edge shift in the dye-sensitized Mg2+-doped TiO2 solar cells", J. Phys. Chem. C 115, 16418-16424 (2011).

xx. R. Gago, A. Redondo-Cubero, M. Vinnichenko, J. Lehmann, F. Munnik, F. J. Palomares. "Spectroscopic evidence of NOx formation and band-gap narrowing in N-doped TiO2 films grown by pulsed magnetron sputtering" Mater. Chem. Phys., 136, 729-736 (2012).

xxx. V. M. Komenko, K. Langer, H. Rager and A. Fett, Phys. Chem. Miner., 1998, 25, 338

SYNOPSIS TOC (Word Style "SN_Synopsis_TOC"). If you are submitting your paper to a journal that requires a synopsis graphic and/or synopsis paragraph, see the Instructions for Authors on the journal's homepage for a description of what needs to be provided and for the size requirements of the artwork.

To format double-column figures, schemes, charts, and tables, use the following instructions:

> Place the insertion point where you want to change the number of columns
> From the **Insert** menu, choose **Break**
> Under **Sections**, choose **Continuous**
> Make sure the insertion point is in the new section. From the **Format** menu, choose **Columns**
> In the **Number of Columns** box, type **1**
> Choose the **OK** button

Now your page is set up so that figures, schemes, charts, and tables can span two columns. These must appear at the top of the page. Be sure to add another section break after the table and change it back to two columns with a spacing of 0.33 in.

Table 1. Example of a Double-Column Table

Column 1	Column 2	Column 3	Column 4	Column 5	Column 6	Column 7	Column 8

Authors are required to submit a graphic entry for the Table of Contents (TOC) that, in conjunction with the manuscript title, should give the reader a representative idea of one of the following: A key structure, reaction, equation, concept, or theorem, etc., that is discussed in the manuscript. Consult the journal's Instructions for Authors for TOC graphic specifications.

Insert Table of Contents artwork here